Electronic Supplementary Material (ESI) for Energy Advances.

Electronic Supplementary Information

Exploring the Feasibility of a Two-Dimensional Layered Cobalt-Based Coordination Polymer for Supercapacitor Applications: Effect of Electrolytic Cations

Rakesh Deka[a], Shashank Rathi[a], and Shaikh M. Mobin[a,b,c*]

[a]Department of Chemistry, [b]Center for Electric Vehicle and Intelligent Transport System (CEVIT), [c]Center of Advanced Electronics (CAE), Indian Institute of Technology Indore, Khandwa Road, Simrol, Indore 453552, India.

Corresponding Author: E-mail: xray@iiti.ac.in Tel: +91 731 6603 336

Physical Measurements

All the reagents and solvents were purchased commercially and used without further purification. The Single crystal data was collected by Agilent Technologies' SUPERNOVA diffractometer using graphite monochromated Mo Kα radiation (λα = 0.71073 Å). Thermogravimetric analysis (TGA) was recorded with a METTLER TOLEDO (TGA/DSC1) system through STARe software by a heating rate of 10 °C/min in an N_2 atmosphere up to 800 °C. For the Powder X-ray diffraction (PXRD) analysis, Cu Kα (0.154 nm) monochromatic radiation was used with a Bruker, D2-Phaser X-ray diffractometer. The morphologies were investigated by a field emission scanning electron microscope (FESEM, JEOL JSM-6500 F). Brunauer−Emmett−Teller (BET) surface area and Barrett−Joyner−Halenda (BJH) distribution determinations were conducted on an Autosorb iQ (Quantachrome Instruments, version 1.11). FT-IR experiment was performed by using Perkin Elmer-Spectrum Two with ATR mode. For the electrochemical study Autolab PGSTAT 204N instrument is utilized with platinum electrode as counter electrode and Ag/AgCl as reference electrode. Carbon Cloth (CC) are used as working electrode along with NOVA (2.1) software for the electrochemical measurement.

X-Ray structural analysis

The single crystal of **Co-CP** is mounted with Agilent Technologies' SUPERNOVA diffractometer using graphite monochromated Mo Kα radiation (λα = 0.71073 Å) at room temperature (293.15 K). Using Olex2[1], the structure was solved with the olex2.solve[2] structure solution program using Charge Flipping and refined with the olex2.refine refinement package using Levenberg-Marquardt minimisation. The Mercury programmed was used to draw the molecular structure, interactions (ver. 3.8).

Experimental

Materials

All chemicals were used without any further purification. The $Co(NO_3)_2.6H_2O$, 5-hydroxyisophthalic acid, dabco(1,4-diazabicyclo[2.2.2]octane), NaOH, KOH, $LiOH.H_2O$, N,N-dimethylformamide (DMF), ethanol, and methanol were purchased from Merck and Sigma Aldrich chemicals. The aqueous electrolytes solutions were prepared by dissolving in de-ionized water.

Synthesis of Co-CP

In a general reaction, 0.3 mmol of 5-hydroxyisophthalic acid (54.63 mg) and 0.3 mmol of dabco (33.65 mg) were dissolved in 5 mL DMF (Solution 1). Afterward, 0.3 mmol of $Co(NO_3)_2 \cdot 6H_2O$ (87.30 mg) was separately dissolved in 5 mL methanol (Solution 2). Later on, 1 mL of solution 1 was placed at the bottom of a crystallization tube, followed by 2 mL of DMF: Methanol (1:1) was placed carefully above solution 1 to form a separate layer. Afterwards, in the crystallization tube 1 mL of solution 2 was added into it to form another layer. The tube was then packed with parafilm and kept at room temperature for a few days. The rose-pink colored crystals of **Co-CP** were observed on the tube wall after a few days of the aging process. The observed crystals were separated and carefully ground into a fine powder with the help of a mortar and pestle and washed several times with DMF, DI water, and ethanol, respectively. Subsequently, the obtained powder was dried at room temperature for further characterization and electrochemical applications.

Electrochemical study

Measurement and Co-CP electrode preparation

Electrochemical studies were carried out to evaluate the supercapacitor efficiency of the material. Mainly, three different techniques were used potentiostat cyclic voltammetry (CV), galvanostatic charge–discharge (GCD), and electrochemical impedance spectroscopy (EIS) for both three and two electrode systems. The electrochemical measurements were performed at room temperature with three conventional electrodes system. The synthesized **Co-CP** was deposited on carbon cloth (1 cm × 1 cm) as the working electrode, platinum wire as the counter electrode, and Ag/AgCl as a reference electrode. At first, the **Co-CP** was dispersed in ethanol and drop cast on the carbon cloth (400 μg), and air dried for electrochemical study.

Evaluation of efficiency

To evaluate the specific capacitance (F g^{-1}) of **Co-CP** following formulae is used:[3]

$$C_s = \frac{I \times \Delta t}{m \times \Delta V} \quad \text{(S1)}$$

Here, the current density, discharge time, and potential window of GCD were assigned by I/m, Δt, and Δ*V,* respectively.

Moreover, the energy density (E) and power density (P) were calculated for the asymmetric supercapacitor following formulae are used:[3]

$$E = \frac{Cs}{2 \times 3.6} \times \Delta V^2 \quad \text{(S2)}$$

$$P = \frac{E}{\Delta t} \times 3600 \quad \text{(S3)}$$

Here, the GCD's specific capacitance, potential window, and discharge time were assigned by C_s, Δ*V*, and Δt, respectively.

Measurement of electrochemical active surface area (EASA)

To measure the EASA of **CO-CP** before and after cyclic stability, the double-layer capacitance (C_{dl}) is determined from the cyclic voltammograms in a non-faradaic region (0.1 V to 0.3 V). To obtain the value of C_{dl}, the current was measured at a fixed potential (0.22 V) from the CV curve which is plotted against the scan rates. The EASA is obtained by using the following formulae:[4]

$$EASA = C_{dl}/C_s \qquad (S4)$$

Here, C_s is the specific capacitance, and C_s values for carbon electrode materials, 0.02 mF/cm^2 are considered for EASA calculation.[4]

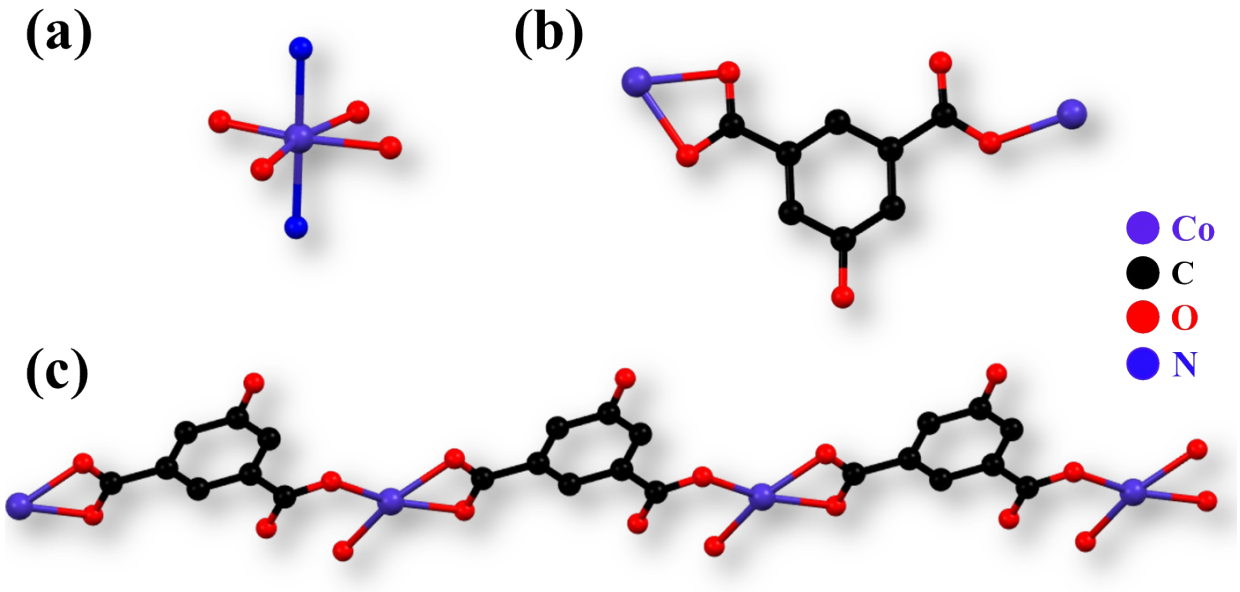

Fig. S1 (a) Distorted octahedral coordination of Co(II) ion, (b) Coordination modes of 5-hydroxyisophthalic acid ((κ1)-(κ1))-μ2, ((κ1) –(κ0)) -μ2, and (c) Ball and stick model showing one-dimensional chain of **Co-CP** view along b-axis.

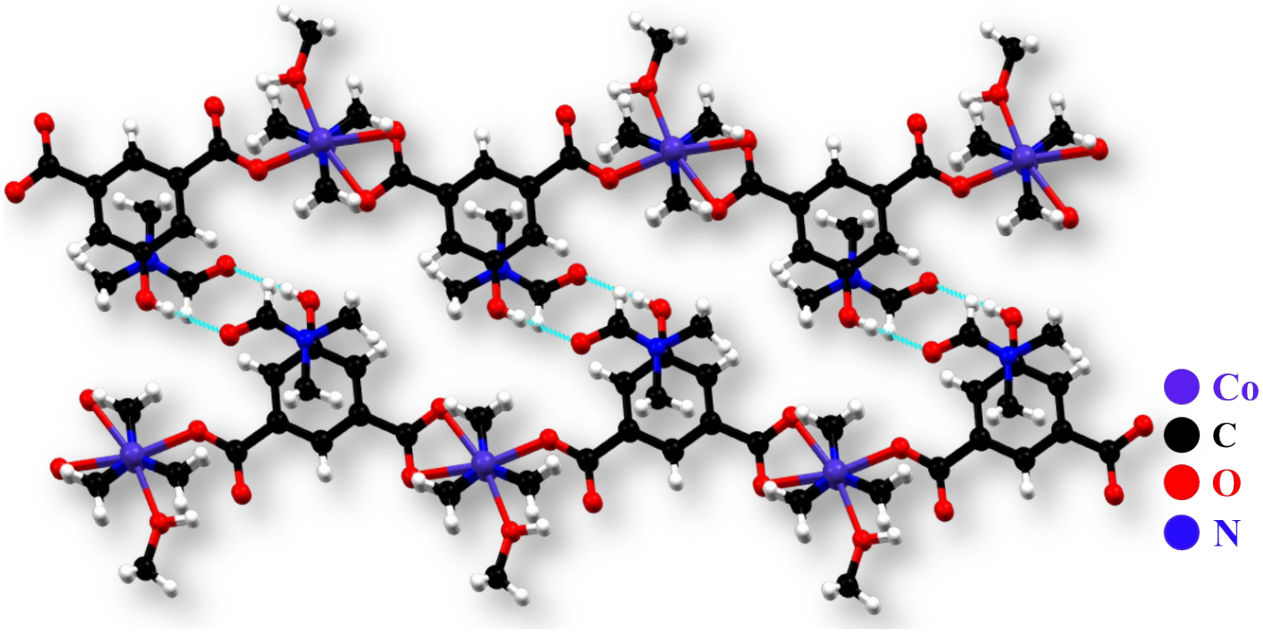

Fig. S2 Ball and stick model showing the hydrogen bonding interaction between the two 2D structure of **Co-CP** view along b axis.

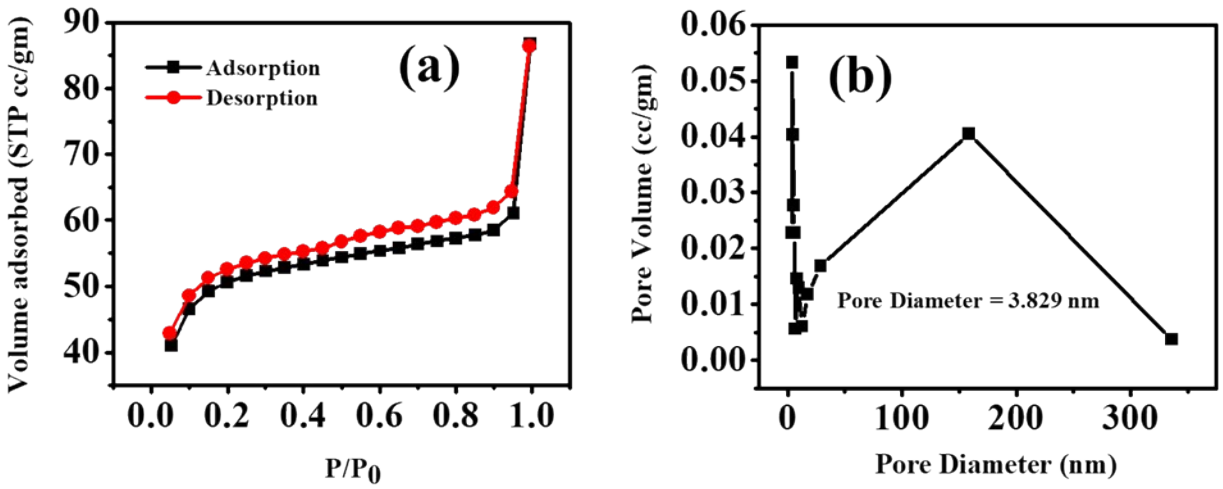

Fig. S3 (a) Nitrogen adsorption desorption isotherm, (b) corresponding pore size distribution of **Co-CP**.

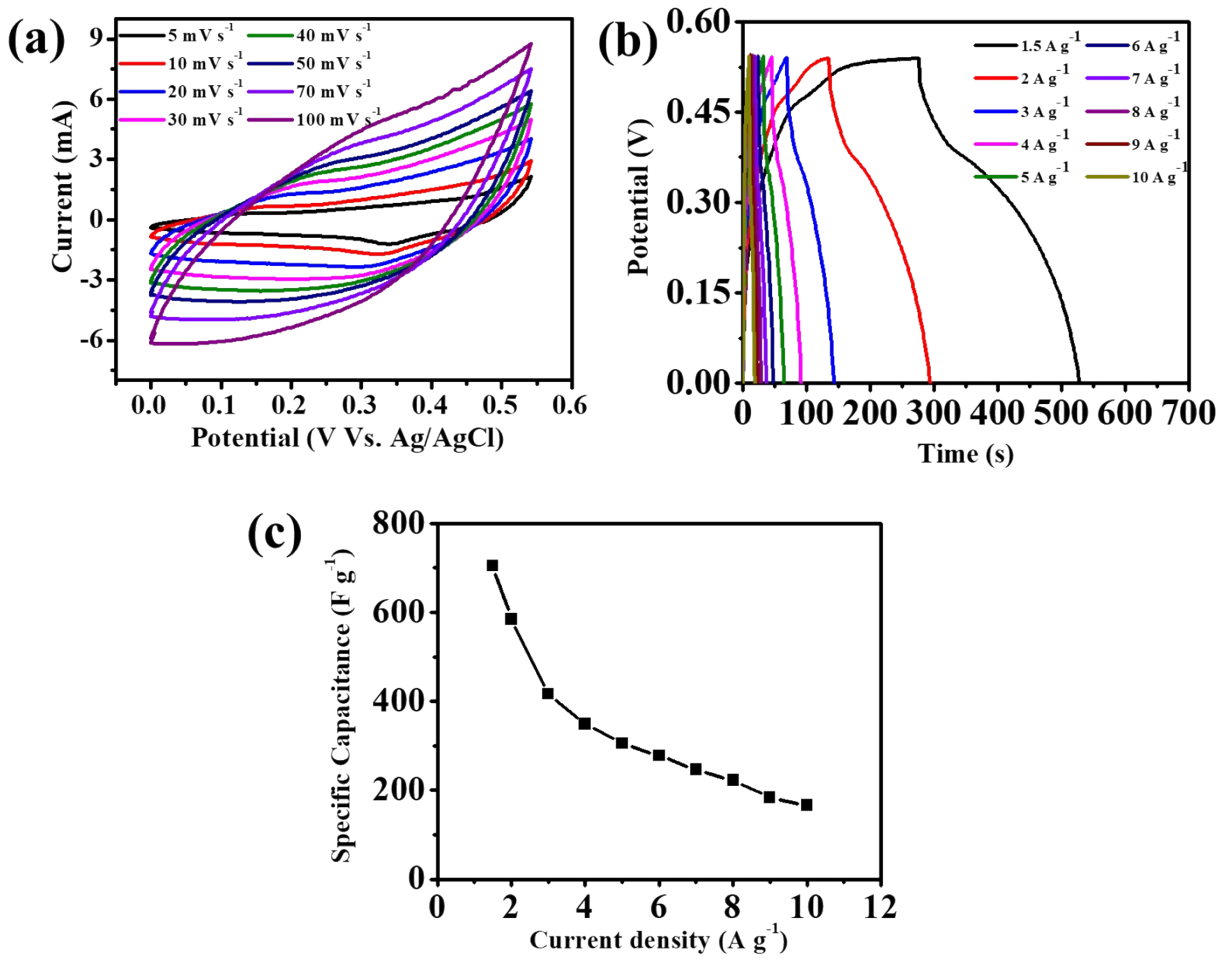

Fig. S4 (a) CV at various scan rates, (b) GCD at different current density, and (c) specific capacitance vs current density in 1M NaOH for **Co-CP**.

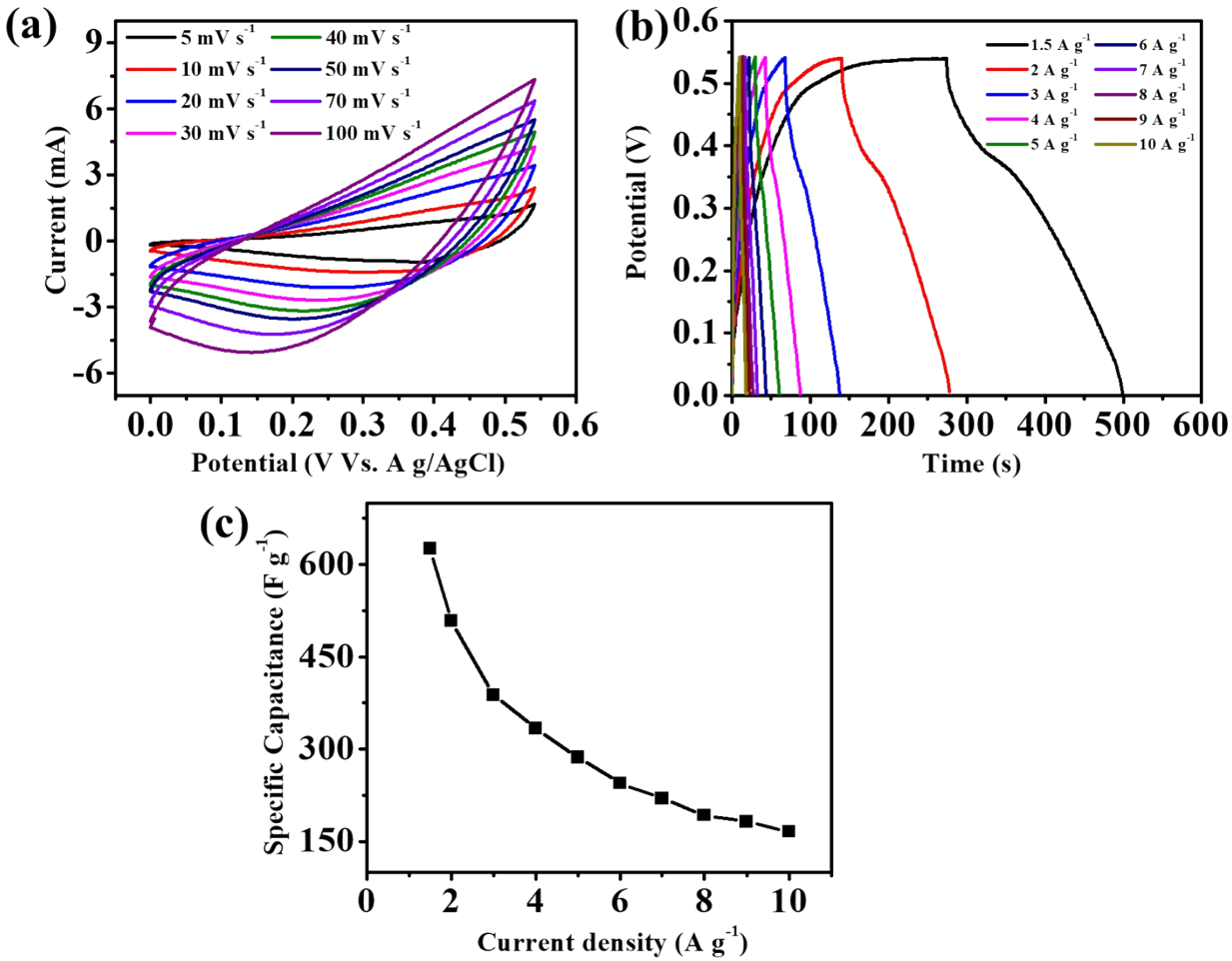

Fig. S5 (a) CV at various scan rates, (b) GCD at different current density, and (c) specific capacitance vs current density in 1M KOH for **Co-CP**.

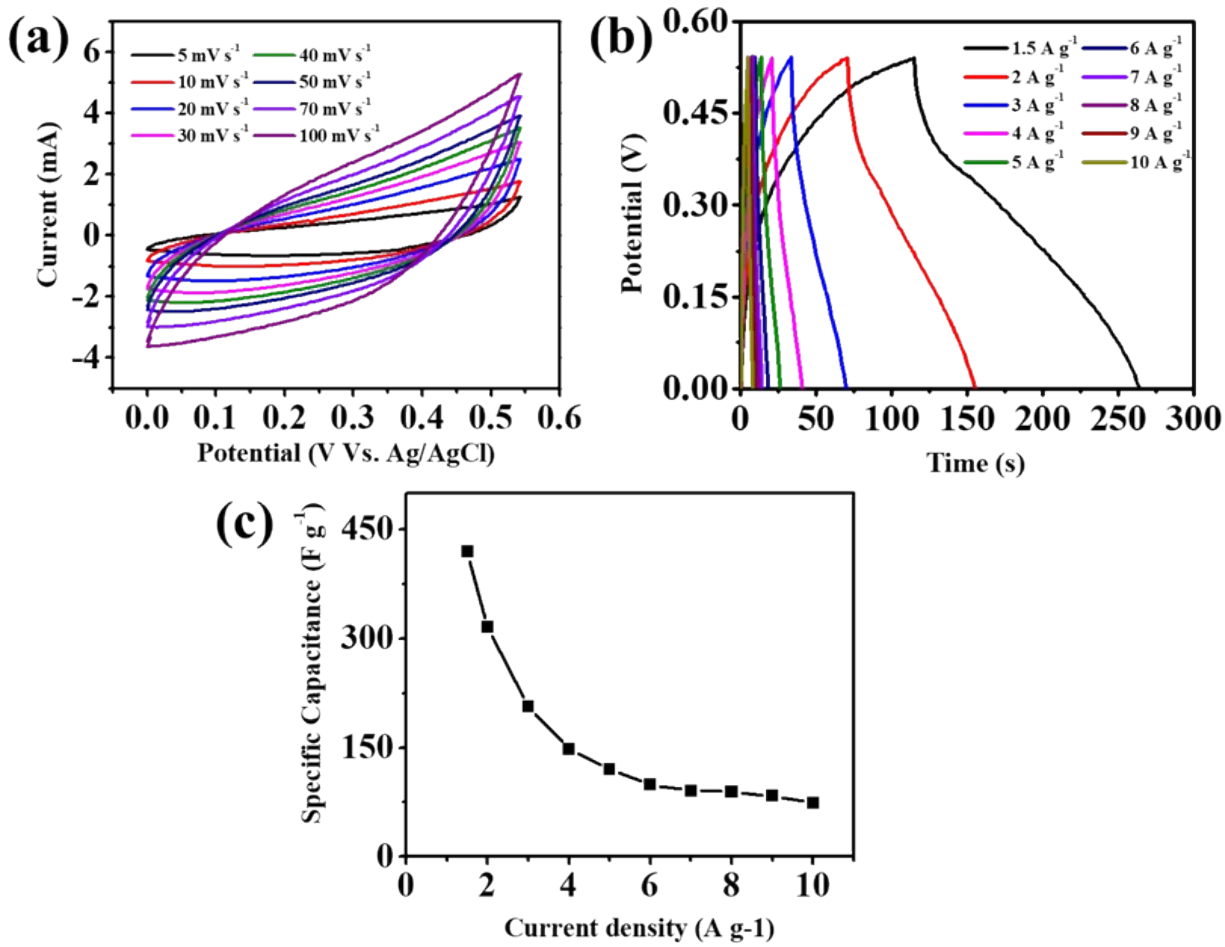

Fig. S6 (a) CV at various scan rates, (b) GCD at different current density, and (c) specific capacitance vs current density in 1M LiOH for **Co-CP**.

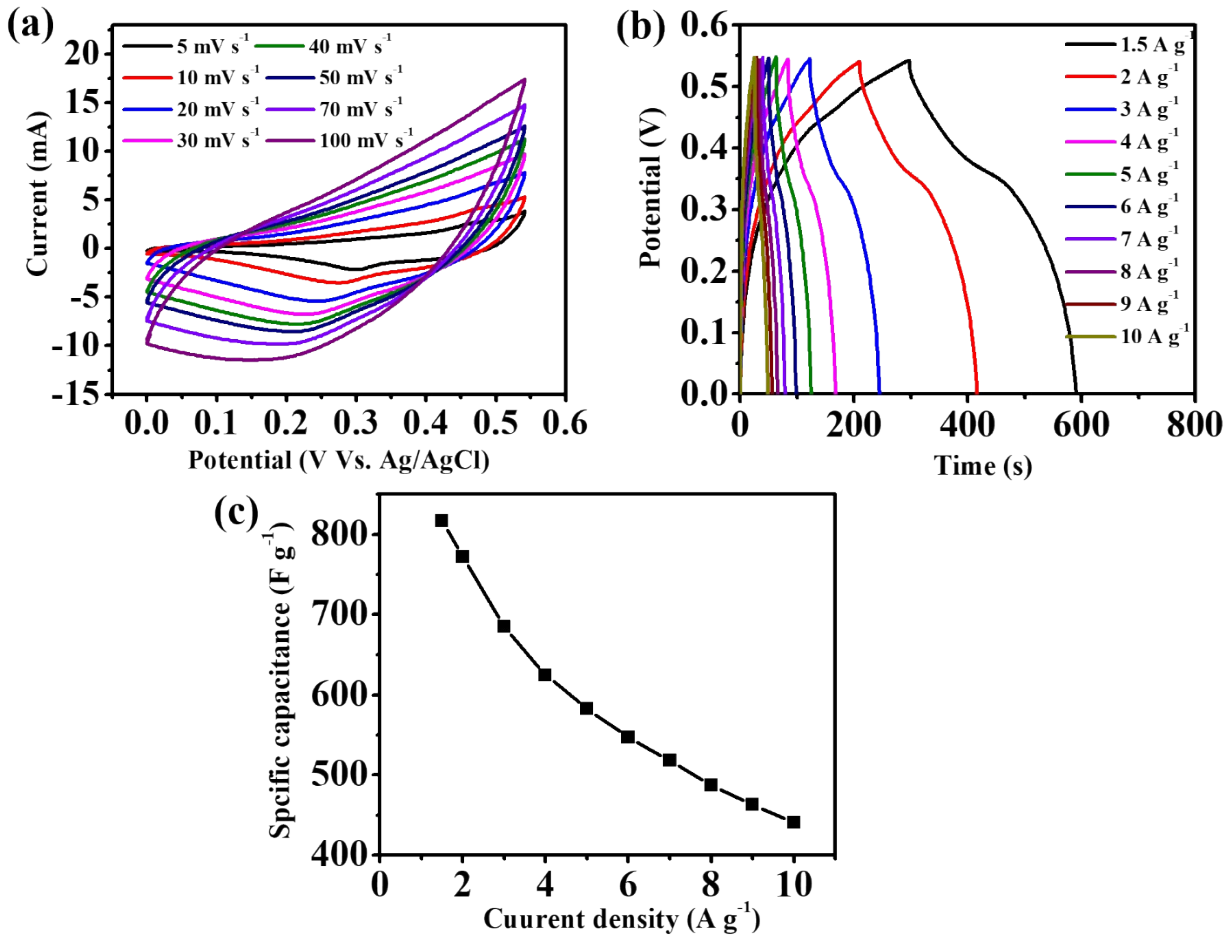

Fig. S7 (a) CV at various scan rates, (b) GCD at different current density, and (c) specific capacitance vs current density in 3M NaOH for **Co-CP**.

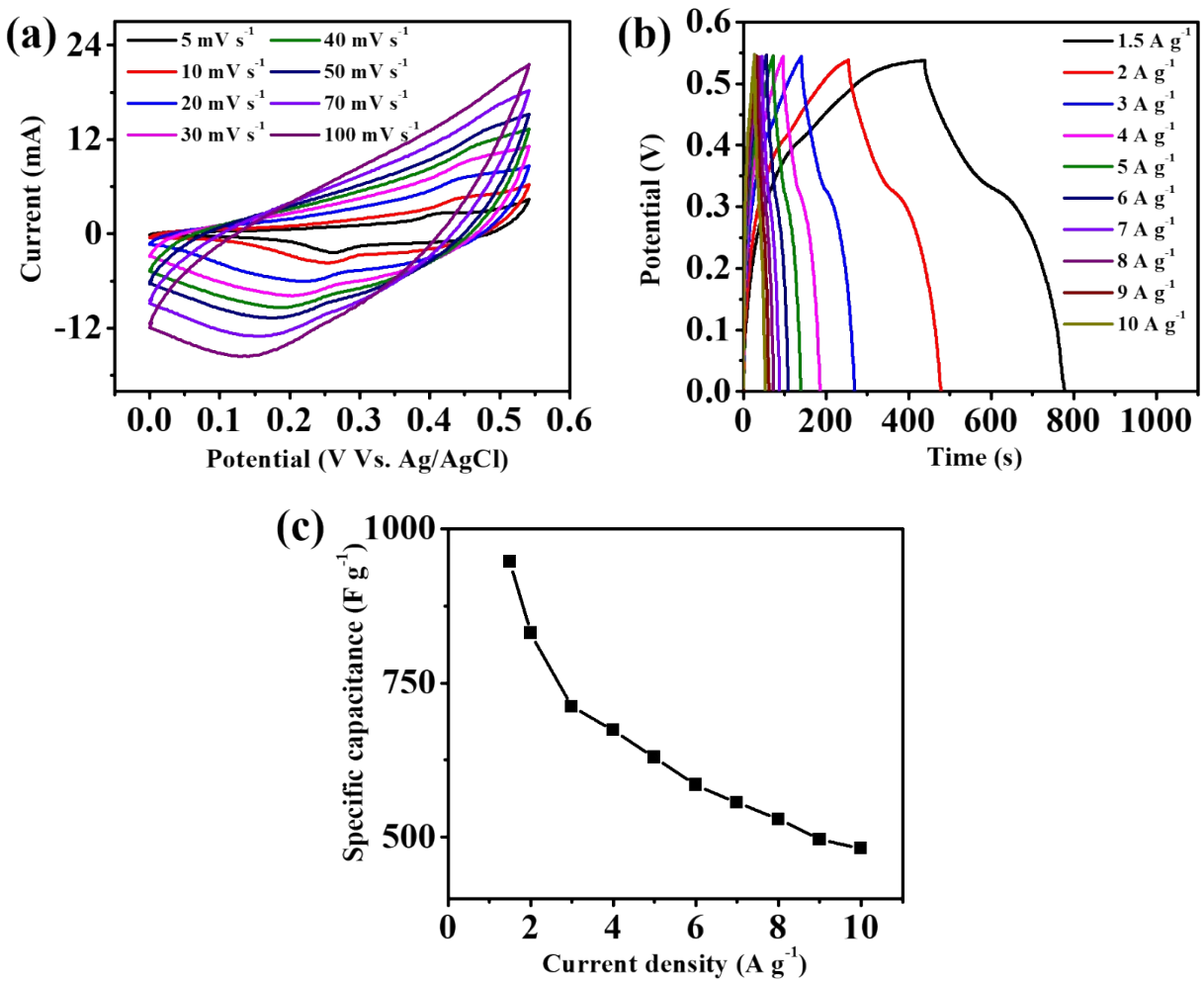

Fig. S8 (a) CV at various scan rates, (b) GCD at different current density, and (c) specific capacitance vs current density in 5M NaOH for **Co-CP**.

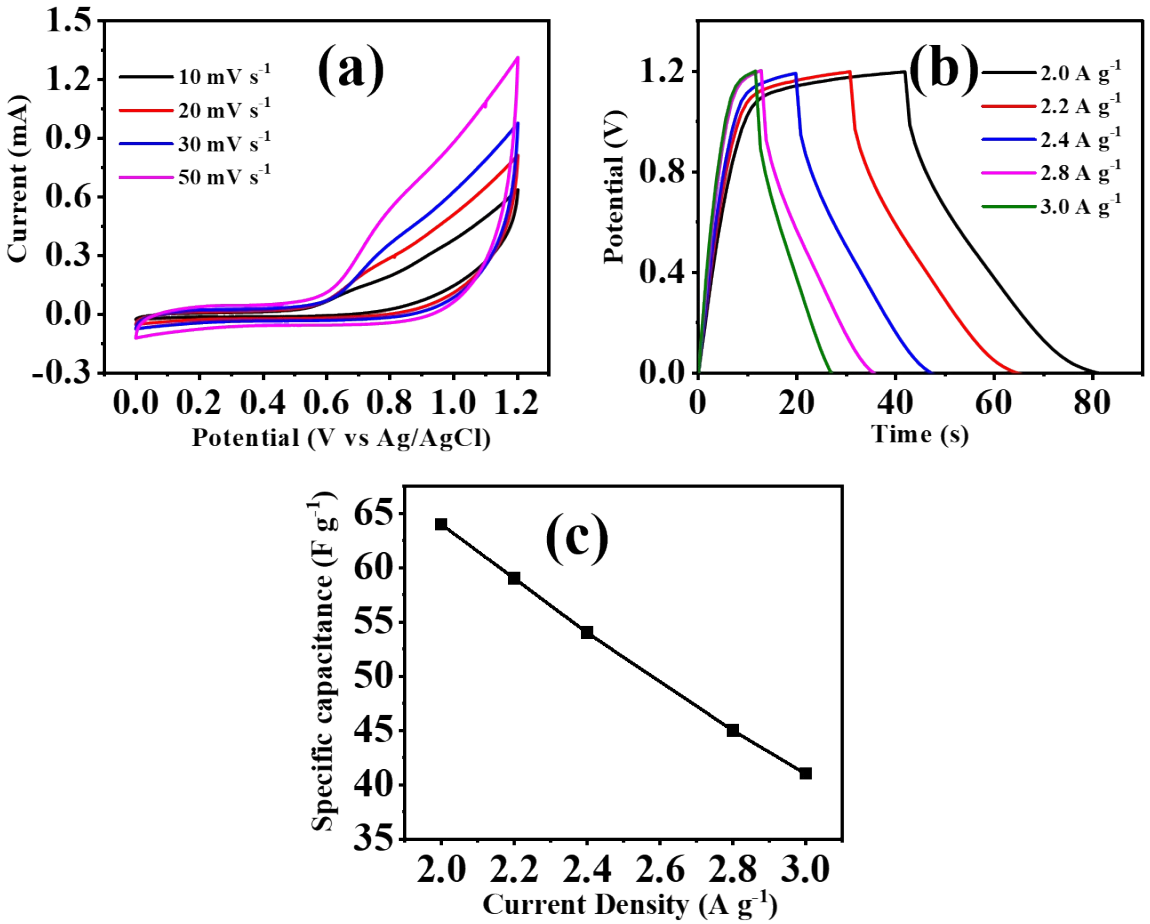

Fig. S9 (a) CV at various scan rates, (b) GCD at different current density, and (c) specific capacitance vs current density for ASC device with KOH-PVA gel of **Co-CP**.

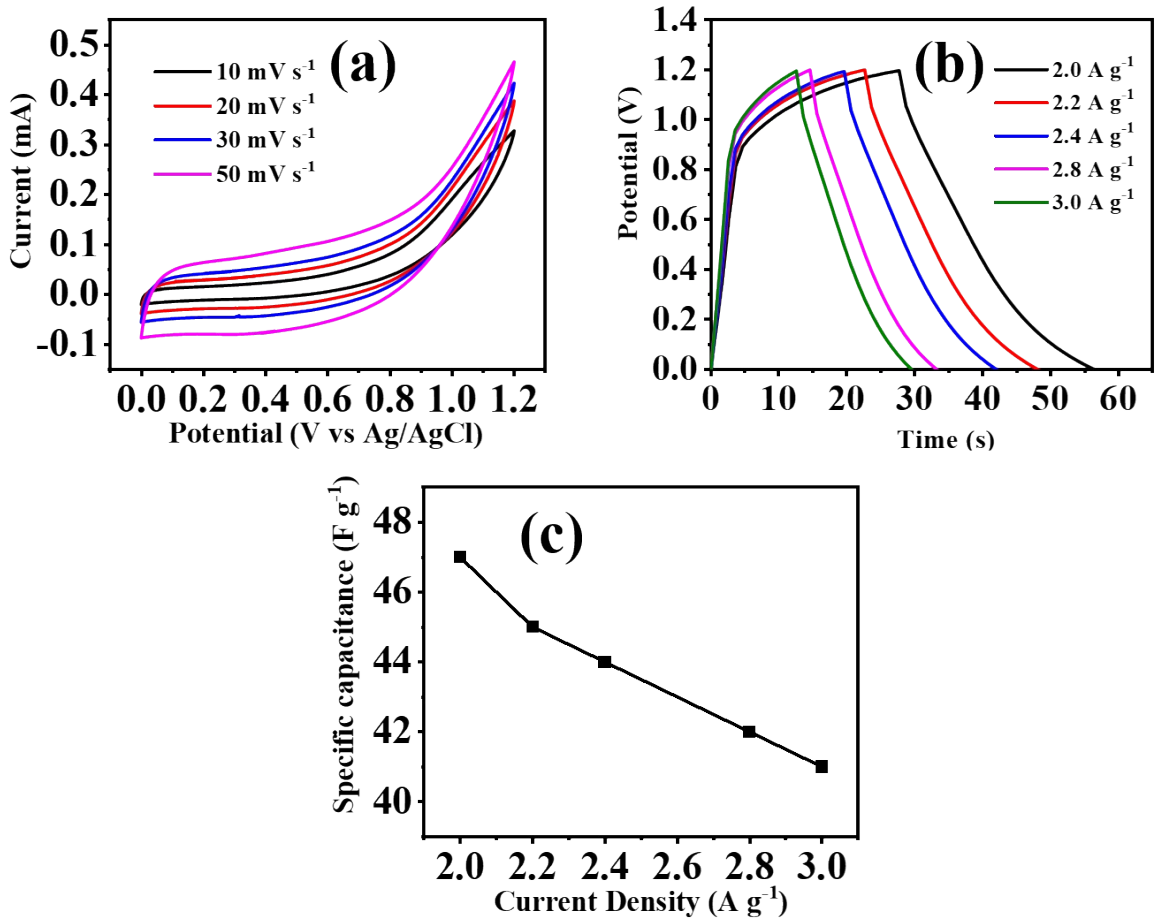

Fig. S10 (a) CV at various scan rates, (b) GCD at different current density, and (c) specific capacitance vs current density for ASC device with LiOH-PVA gel of **Co-CP**.

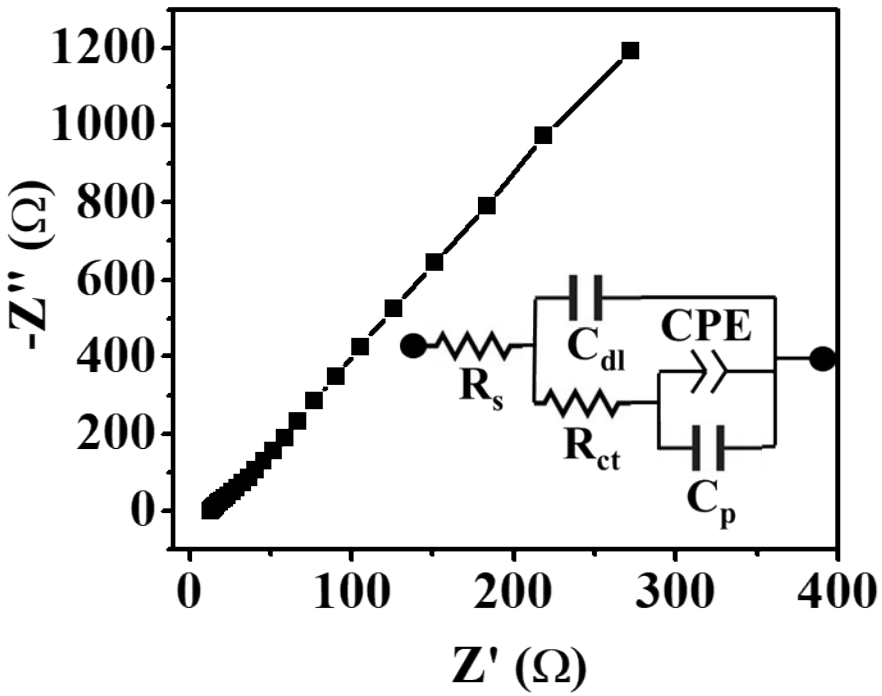

Fig. S11 Nyquist plot for ASC device of **Co-CP** NaOH-PVA gel.

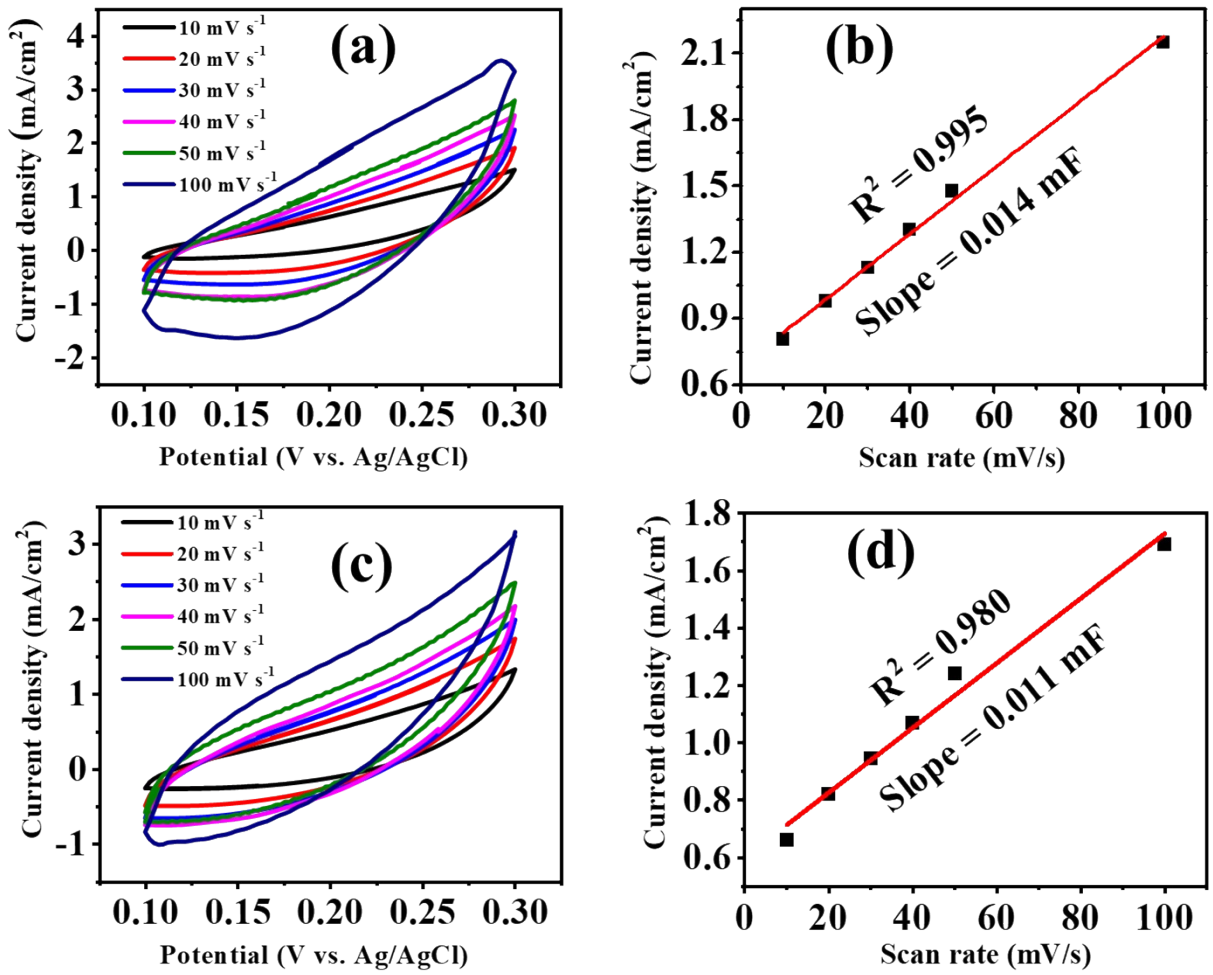

Fig. S12 CV curves in a non-faradaic region (0.1 to 0.3 V vs. Ag/AgCl) at scan rates of 10, 20, 30, 40, 50, 100 mV/s for (a) CV before cyclic stability measurement, (b) corresponding linear regression between the current density and scan rates, (c) CV after cyclic stability measurement, and (d) corresponding linear regression between the current density and scan rates.

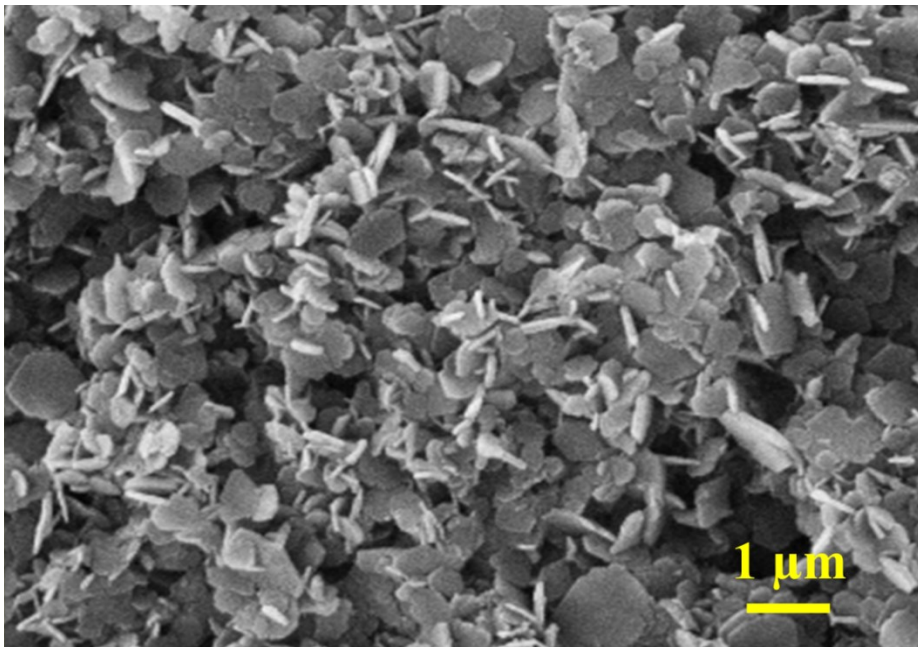

Fig. S13 SEM images of Co-CP after the cyclic stability measurement.

Table S1 Bond length and bond angle of **Co-CP**.

Bond lengths (Å)			
Co(1)-O(1)	2.050(3)		
Co(1)-O(1)	2.050(3)		
Co(1)-O(111)	2.083(3)		
Co(1)-O(5)#1	2.126(3)		
Co(1)-O(4)#1	2.186(3)		
Co(1)-N(1)	2.272(2)		
Co(1)-N(1)#2	2.272(2)		
Co(1)-C(2)#1	2.482(4)		
Co(1)-O(111)	2.083(3)		
Co(1)-O(5)#1	2.126(3)		
Co(1)-O(4)#1	2.186(3)		
Co(1)-N(1)	2.272(2)		
Co(1)-N(1)#2	2.272(2)		
Co(1)-C(2)#1	2.482(4)		
Bond angle (°)			
O(1)-Co(1)-O(111)	90.71(13)	O(1)-Co(1)-O(111)	90.71(13)
O(1)-Co(1)-O(5)#1	105.21(11)	O(1)-Co(1)-O(5)#1	105.21(11)
O(111)-Co(1)-O(5)#1	164.08(12)	O(111)-Co(1)-O(5)#1	164.08(12)
O(1)-Co(1)-O(4)#1	166.45(12)	O(1)-Co(1)-O(4)#1	166.45(12)
O(111)-Co(1)-O(4)#1	102.84(12)	O(111)-Co(1)-O(4)#1	102.84(12)
O(5)#1-Co(1)-O(4)#1	61.24(11)	O(5)#1-Co(1)-O(4)#1	61.24(11)
O(1)-Co(1)-N(1)	89.62(6)	O(1)-Co(1)-N(1)	89.62(6)
O(111)-Co(1)-N(1)	90.09(6)	O(111)-Co(1)-N(1)	90.09(6)
O(5)#1-Co(1)-N(1)	90.02(6)	O(5)#1-Co(1)-N(1)	90.02(6)
O(4)#1-Co(1)-N(1)	90.35(6)	O(4)#1-Co(1)-N(1)	90.35(6)
O(1)-Co(1)-N(1)#2	89.62(6)	O(1)-Co(1)-N(1)#2	89.62(6)
O(111)-Co(1)-N(1)#2	90.09(6)	O(111)-Co(1)-N(1)#2	90.09(6)
O(5)#1-Co(1)-N(1)#2	90.02(6)	O(5)#1-Co(1)-N(1)#2	90.02(6)

O(4)#1-Co(1)-N(1)#2	90.35(6)	O(4)#1-Co(1)-N(1)#2	90.35(6)
N(1)-Co(1)-N(1)#2	179.23(13)	N(1)-Co(1)-N(1)#2	179.23(13)
O(1)-Co(1)-C(2)#1	136.02(13)	O(1)-Co(1)-C(2)#1	136.02(13)
O(111)-Co(1)-C(2)#1	133.27(14)	O(111)-Co(1)-C(2)#1	133.27(14)
O(5)#1-Co(1)-C(2)#1	30.81(13)	O(5)#1-Co(1)-C(2)#1	30.81(13)
O(4)#1-Co(1)-C(2)#1	30.43(13)	O(4)#1-Co(1)-C(2)#1	30.43(13)
N(1)-Co(1)-C(2)#1	90.21(6)	N(1)-Co(1)-C(2)#1	90.21(6)
N(1)#2-Co(1)-C(2)#1	90.21(6)	N(1)#2-Co(1)-C(2)#1	90.21(6)
C(1)-O(1)-Co(1)	129.4(3)	C(1)-O(1)-Co(1)	129.4(3)
C(2)-O(4)-Co(1)#4	87.9(2)	C(2)-O(4)-Co(1)#4	87.9(2)
C(2)-O(5)-Co(1)#4	90.3(2)	C(2)-O(5)-Co(1)#4	90.3(2)
C(10)-N(1)-Co(1)	112.06(19)	C(10)-N(1)-Co(1)	112.06(19)
C(11)-N(1)-Co(1)	112.24(19)	C(11)-N(1)-Co(1)	112.24(19)
C(9)-N(1)-Co(1)	112.28(18)	C(9)-N(1)-Co(1)	112.28(18)

Table S2 Specific capacitance values in different electrolytes (NaOH, KOH, LiOH)

Current density ($A\ g^{-1}$)	**Specific capacitance ($F\ g^{-1}$)**		
	1M NaOH	**1M KOH**	**1M LiOH**
1.5	706	625	420
2	586	508	315
3	417	388	207
4	349	333	148
5	306	286	120
6	278	244	99
7	246	220	91
8	222	192	89
9	183	182	83
10	167	166	74

Table S3 Nyquist plot fitting parameter in three electrode system.

Elements	**NaOH**	**KOH**	**LiOH**
R_s (Ω)	7.45	8.60	11.2
R_{ct} (Ω)	6.99	3.16	9.97
C_{dl} (μF)	2.01	1.89	9.80
C_p (fF)	900	900	900
W (mMho*s^1/2)	15.1	10.5	11.5

Table S4 Specific capacitance values in different gel system for ASC device of **Co-CP**.

Current density (A g^{-1})	**Specific capacitance (F g^{-1})**		
	NaOH-PVA	**KOH-PVA**	**LiOH-PVA**
2.0	85	64	47
2.2	73	59	45
2.4	66	54	44
2.8	53	45	42
3.0	50	42	41

Table S5 Nyquist plot fitting parameter in two electrode system in NaOH-PVA gel.

Elements	**NaOH-PVA**
R_s (Ω)	12.9
R_{ct} (mΩ)	50.6
C_{dl} (fF)	900
C_p (fF)	900
W (mMho*s^N)	1.28 (N= 0.853)

References

1 O. V. Dolomanov, L. J. Bourhis, R. J. Gildea, J. A. K. Howard and H. Puschmann, *J Appl Crystallogr*, 2009, **42**, 339–341.

2 L. J. Bourhis, O. V. Dolomanov, R. J. Gildea, J. A. K. Howard and H. Puschmann, *Acta Crystallogr A Found Adv*, 2015, **71**, 59–75.

3 R. Deka, R. Rajak, V. Kumar and S. M. Mobin, *Inorg Chem*, 2023, **62**, 3084–3094.

4 A. Valipour, N. Hamnabard, S. M. H. Meshkati, M. Pakan and Y.-H. Ahn, Dalton Trans., 2019, **48**, 5429–5443.